Inorg. Chem. **2007**, *46*, 7756–7766

Tuning *Inter*molecular Magnetic Exchange Interactions in the Solids $C_xF_{2x}(CNSSS)_2(AsF_6)_2$: Structural, EPR, and Magnetic Characterization of Dimeric ($x = 2$, 4) Diradicals

Andreas Decken,[†] Mohammad Ebdah,[§] Radoslaw M. Kowalczyk,[||] Christopher P. Landee,[§] Eric J. L. McInnes,[||] Jack Passmore,*[,†] Konstantin V. Shuvaev,[†] and Laurence K. Thompson[‡]

Department of Chemistry, University of New Brunswick, Fredericton E3B 6E2, Canada, Department of Physics, Clark University, Worcester, Massachusetts 01610-1477, EPSRC Multi-Frequency EPR Centre, School of Chemistry, The University of Manchester, M13 9PL, U.K., and Department of Chemistry, Memorial University of Newfoundland, St. John's A1B 3X7, Canada

Received December 27, 2006

A series of diradical containing salts $C_xF_{2x}(CNSSS)_2^{\bullet\bullet 2+}(AsF_6^-)_2$ {$x = 2$, **1**[AsF_6]$_2$; $x = 3$, **3**[AsF_6]$_2$; $x = 4$, **2**[AsF_6]$_2$} have been prepared. **1**[AsF_6]$_2$ and **2**[AsF_6]$_2$ were fully characterized by X-ray, variable-temperature magnetic susceptibility, and solid-state EPR measurements, further allowing us to extend the number of examples of the family of rare 7π RCNSSS$^{\bullet+}$ radical cations. **1**[AsF_6]$_2$: $a = 6.5314(7)$ Å, $b = 7.5658(9)$ Å, $c = 9.6048(11)$ Å, $\alpha = 100.962(2)°$, $\beta = 96.885(2)°$, $\gamma = 107.436(2)°$, triclinic, space group $P\bar{1}$, $Z = 1$, $T = 173$ K. **2**[AsF_6]$_2$: $a = 10.6398(16)$ Å, $b = 7.9680(11)$ Å, $c = 12.7468(19)$ Å, $\beta = 99.758(2)°$, monoclinic, space group $P2_1/c$, $Z = 2$, $T = 173$ K. In the solid-state, $C_xF_{2x}(CNSSS)_2^{\bullet\bullet 2+}$ ($x = 2$, 4) formed one-dimensional polymeric chains of dications containing discrete centrosymmetric radical pairs in which radicals were linked by four centered two-electron π^*–π^* bonds [**1**$^{2+}$, d(S···S) = 3.455(1) Å; **2**$^{2+}$, d(S···S) = 3.306(2) Å]. The exchange interactions in these bonds were determined to be –500 ± 30 and –900 ± 90 cm^{-1}, by variable temperature magnetic susceptibility measurements, respectively, providing rare experimental data on the singlet–triplet gaps in the field of thiazyl radicals. For **2**[AsF_6]$_2$, the thermally excited triplet state was unambiguously characterized by EPR techniques [$|D| = 0.0254(8)$ cm^{-1}, $|E| = 0.0013(8)$ cm^{-1}]. These experimental data implied a weakly associated nature of the radical moieties contained in the solids **1**[AsF_6]$_2$ and **2**[AsF_6]$_2$. Computational analysis of the dimerization process is presented, and we show that the 2c 4 electron π^*–π^* bonds in **1**[AsF_6]$_2$ and **2**[AsF_6]$_2$ have ca. 50% and 40% diradical character, respectively. In contrast, **3**[AsF_6]$_2$·SO_2, containing diradical $C_3F_6(CNSSS)_2^{\bullet\bullet 2+}$ with an odd number of CF_2 spacers, showed magnetic behavior that was consistent with the presence of monomeric radical centers in the solid state.

1. Introduction

Over the past 30 years it has been shown that the stable 7π thiazyl radicals exhibit interesting and unprecedented physical properties in the solid state, that is, conductivity, ferromagnetism, and bistability.[1–3] Enhanced communication between thiazyl radical centers, a necessary requirement for cooperative phenomena, propagates via polar $S^{\delta+}\cdots N^{\delta-}$ contacts, as well as other electrostatic and $\pi^*-\pi^*$ interactions. The magnitude of these close interactions, expressed in magnetochemical terms, can vary from very weak ($|2J| < 1$ cm^{-1}) to very strong ($|2J| > 1000$ cm^{-1}), depending on the solid-state structure.[1e] In the latter situation, radical

* To whom correspondence should be addressed. E-mail: passmore@unb.ca. Phone: 1-506-453-4821. Fax: 1-506-453-4981.
[†] Department of Chemistry, University of New Brunswick.
[§] Department of Physics, Clark University.
[||] EPSRC Multi-Frequency EPR Centre, University of Manchester.
[‡] Department of Chemistry, Memorial University of Newfoundland.

(1) (a) Rawson, J. M.; Palacio, F. *Struct. Bonding* **2001**, *100*, 93. (b) Rawson, J. M.; Banister, A. J.; Lavender, I. *Adv. Heterocycl. Chem.* **1995**, *62*, 137. (c) Oakley, R. T. *Adv. Mater.* **1994**, *6*, 798. (d) Rawson, J. M.; Alberola, A.; Whalley, A. *J. Mater. Chem.* **2006**, *16*, 2560. (e) Rawson, J. M.; Luzon, J.; Palacio, F. *Coord. Chem. Rev.* **2005**, 2631.

(2) (a) Cameron, T. S.; Lemaire, M. T.; Passmore, J.; Rawson, J. M.; Shuvaev, K. V.; Thompson, L. K. *Inorg. Chem.* **2005**, *44*, 2576. (b) Du, H.; Haddon, R. C.; Krossing, I.; Passmore, J.; Rawson, J. M.; Schriver, M. J. *Chem. Commun*. **2002**, 1836. (c) Parsons, S.; Passmore, J. *Acc. Chem. Res.* **1994**, *27*, 101.

(3) (a) Rawson, J. M.; McManus, G. D. *Coord. Chem. Rev.* **1999**, *189*, 135. (b) Fujita, W.; Awaga, K.; Takahashi, M.; Takeda, M.; Yamazaki, T. *Chem. Phys. Lett.* **2002**, *362*, 97. (c) Fujita, W.; Awaga, K. *Science* **1999**, *286*, 261.

10.1021/ic062475i CCC: $37.00
Published on Web 08/24/2007

dimerization has occurred with a strong overlap of the respective SOMOs via $\pi^*-\pi^*$ interactions.[4] Recently, we succeeded in determining the singlet−triplet gap (intramolecular exchange interaction $2J$), which is proportional to the intrinsic dimerization energy, of the related thiazyl radical cationic pair, $[ClCNSSS]_2^{2+}$, using the very sensitive EPR technique, and obtained $2J$ as -1900 ± 200 cm^{-1}.[8a] Despite such a large singlet−triplet splitting, the triplet excited-state was sufficiently populated at room temperature (RT) to be observable by solid-state EPR.

It is noteworthy that the $RCNSSS^{\bullet+}$ radical cations belong to a novel class of thiazyl radicals that are predominantly paramagnetic in the solid state and exhibit a wide range of magnetic exchange interactions. For instance, $^{+\bullet}SSSNC-CNSSS^{\bullet+}$ $(Sb_2F_{11}^-)_2$[9c] and $F_3CCNSSS^{\bullet+}AsF_6^-$[8b] contain very weakly interacting radical cations with interradical exchange, $2J$ values of approximately -5 and -4 cm^{-1}, respectively. On the other hand, the magnitude of magnetic exchange is one order larger in $RCNSSS^{\bullet+}AsF_6-$ ($R = Cl_3C$, $2J = -68$ cm^{-1}; $R = F_5C_2$, $2J = -42$ cm^{-1})[8c] and $^{+\bullet}SSSNC-CNSSS^{\bullet+}$-$(MF_6^-)_2$ ($M = As$, $2J = -60$ cm^{-1}; $M = Sb$, $2J = -63$ cm^{-1}).[9c] In another limiting case, the magnetic coupling is very strong reaching -1900 cm^{-1} in $[ClCNSSS]_2^{2+}$ dimers.[8a] These results imply that a minor modification of the substituent group in the $RCNSSS^{\bullet+}$ ring systems leads to significant changes in the magnitude of magnetic exchange interaction (e.g., from -5 to -1900 cm^{-1} for $R = F_3C$ and Cl, respectively).

Chart 1

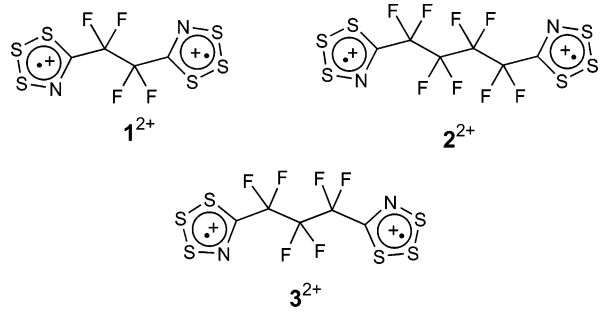

To further explore the relationship between magnetic properties, the extent of magnetic coupling, and the overall structure, we have prepared and characterized diradical salts of the general formula $^{+\bullet}SSSNC-[spacer]-CNSSS^{\bullet+}$. The other examples of diradicals containing two $-CNSSS^{\bullet+}$ rings are the AsF_6^- salts of $^{+\bullet}SSSNC(Z)CNSSS^{\bullet+}$ ($Z = CO$, CCl_2),[10] as well as MF_6^- ($M = As$, Sb) and $Sb_2F_{11}^-$ salts of the planar $^{+\bullet}SSSNC-CNSSS^{\bullet+}$.[9] The latter dication does not adopt the expected closed-shell Lewis structure but rather contains a C−C single bond and two unpaired electrons, which are only very weakly interacting. Salts of $^{+\bullet}SSSNC-CNSSS^{\bullet+}$ are the only examples, other than dioxygen, of nonsterically hindered main group diradicals that are paramagnetic in the solid state.

The incorporation of spacers between two radical moieties in $^{+\bullet}SSSNC-[spacer]-CNSSS^{\bullet+}$ inhibits *intra*molecular coupling and thus allows us to focus exclusively on *inter*molecular interaction between radical centers in the solid state, enabling us to trace structural and magnetic property changes as a function of spacer size. Specifically, we targeted the AsF_6^- salts of polyfluorinated diradicals, namely, $^{+\bullet}(SSSNC)C_2F_4(CNSSS)^{\bullet+}$ ($\mathbf{1}^{2+}$), $^{+\bullet}(SSSNC)C_4F_8(CNSSS)^{\bullet+}$ ($\mathbf{2}^{2+}$), and $^{+\bullet}(SSSNC)C_3F_6(CNSSS)^{\bullet+}$ ($\mathbf{3}^{2+}$) (Chart 1). It was observed that the derivatives with an even number of carbon atoms ($\mathbf{1}^{2+}$ and $\mathbf{2}^{2+}$) associated into radical pairs with large exchange interactions, while magnetic measurements indicated that $\mathbf{3}^{2+}$ was paramagnetic because of its much weaker magnetic coupling between radical centers. Herein, we provide a full account on the X-ray structures, solid-state EPR, and magnetic properties of $\mathbf{1}[AsF_6]_2$ and $\mathbf{2}[AsF_6]_2$ and the magnetic data for $\mathbf{3}[AsF_6]_2 \cdot SO_2$.

2. Experimental Section

2.1. Materials. NCC_2F_4CN, NCC_4F_8CN, and $H_5C_2OOCC_3F_6$-$COOC_2H_5$ were obtained from SynQuest and were used as received. The mixture of $S_4(AsF_6)_2$ and $S_8(AsF_6)_2$ (1:1 ratio) was prepared by condensing AsF_5 and traces of Br_2 onto S_8 (vacuum-dried) in the appropriate mole ratio in liquid SO_2, as previously described.[11a] SO_2 (Liquid Air, 99.9998%) was distilled onto CaH_2 and stored for at least 24 h prior to use.

(4) Determination of the small dimerization energies in sulfur nitrogen radicals is nontrivial. In solution, the dimerization energies include solvation energies of the respective monomer and dimer which may not cancel each other out. By variable-temperature EPR, values from 0 kJ mol^{-1} for $F_3CCSNSCCF_3$ (ref 5a) to -19 kJ mol^{-1} for $PhCNSNS^{\bullet}$ (ref 6a) and -35 kJ mol^{-1} for $PhCNSSN^{\bullet}$ (ref 6b) have been determined in solution. Gas-phase calculated values can be obtained, but often the dimer is not completely isolated in the solid state but is further stabilized by interdimer interactions, for example, $[C_6H_4SNS]_2$ (ref 7a) and $F_3CCSNSCCF_3$, which seems not to exist as a dimer (calculations) but is stabilized as a tetramer in the solid state (ref 5b). A full determination of thermodynamic properties giving entropies and enthalpies of fusion, vaporization, and sublimation have been obtained in some cases and imply very small dimerization energies, for example, for $F_3CCSNSCCF_3$ (ref 5b) and $RCNSSN^{\bullet}$ ($R = CH_3$, ref 7b; Ph, ref 6b; *t*-Bu, ref 7c).

(5) (a) Awere, E. G.; Burford, N.; Mailer, C.; Passmore, J.; Schriver, M. J.; White, P. S.; Banister, A. J.; Oberhammer, H.; Sutcliffe, L. H. *J. Chem. Soc., Chem. Commun.* **1987**, 66. (b) Brownridge, S.; Du, H.; Fairhurst, S. A.; Haddon, R. C.; Oberhammer, H.; Parsons, S.; Passmore, J.; Schriver, M. J.; Sutcliffe, L. H.; Westwood, N. P. C. *J. Chem. Soc., Dalton Trans.* **2000**, 3365.

(6) (a) Passmore, J.; Sun, X. *Inorg. Chem.* **1996**, *35*, 1313. (b) Fairhurst, S. A.; Johnson, K. M.; Sutcliffe, L. H.; Preston, K. F.; Banister, A. J.; Hauptman, Z. V.; Passmore, J. *J. Chem. Soc., Dalton Trans.* **1986**, 1465.

(7) (a) Awere, E. G.; Burford, N.; Haddon, R. C.; Parsons, S.; Passmore, J.; Waszczak, J. V.; White, P. S. *Inorg. Chem.* **1990**, *29*, 4821. (b). MacLean, G. K.; Passmore, J.; Rao, M. N. S.; Schriver, M. J.; White, P. S.; Bethell, D.; Pilkington, R. S.; Sutcliffe, L. H. *J. Chem. Soc., Dalton Trans.* **1985**, 1405. (c) Brooks, W. V. F.; Burford, N.; Passmore, J.; Schriver, M. J.; Sutcliffe, L. H. *J. Chem. Soc., Chem. Commun.* **1987**, 69.

(8) (a) Cameron, T. S.; Decken, A.; Kowalczyk, R. M.; McInnes, E. J. L.; Passmore, J.; Rawson, J. M.; Shuvaev, K. V.; Thompson, L. K. *Chem. Commun.* **2006**, 2277. (b) Cameron, T. S.; Haddon, R. C.; Mattar, S. M.; Parsons, S.; Passmore, J.; Ramirez, A. P. *Inorg. Chem.* **1992**, *31*, 2274. (c) Decken, A.; Mattar, S. M.; Passmore, J.; Shuvaev, K. V.; Thompson, L. K. *Inorg. Chem.* **2006**, *45*, 3878.

(9) (a) Boyle, P. D.; Parsons, S.; Passmore, J.; Wood, D. J. *J. Chem. Soc., Chem. Commun.* **1993**, 199. (b) Enright, G. D.; Morton, J. R.; Passmore, J.; Preston, K. F.; Thompson, R. C.; Wood, D. J. *Chem. Commun.* **1996**, 967. (c) Cameron, T. S.; Decken, A.; Grein, F.; Kowalczyk, R. M.; Knapp, C.; Passmore, J.; Rautiainen, J. M.; Shuvaev, K. V.; Thompson, R. C.; Wood, D. J. Unpublished work. (d) Cameron, T. S.; Decken, A.; Fang, M.; Parsons, S.; Passmore, J.; Wood, D. J. *Chem. Commun.* **1999**, 1801.

(10) Cameron, T. S.; Knapp, C.; Parsons, S.; Passmore, J.; Rivard, E.; Shuvaev, K. V.; Thompson, L. K.; Thompson, R. C. Unpublished work.

2.2. General Procedures. All reactions were performed in two-bulb, two-valve Pyrex vessels incorporating 25 mL bulbs, using techniques that that allow manipulation of volatile materials quantitatively in a closed system, as described previously.[11b] Solid reagents and crystals were manipulated and handled MBraun Unilab 1200/700 drybox. FT-IR spectra of Nujol mulls between KBr disks were recorded on a Thermo Nicolet FT-IR 470 spectrometer (32 scans, resolution 2.0 cm^{-1}). The X-band EPR spectra were recorded using a Bruker ESP300E spectrometer with microwave bridges in conjunction with Bruker dielectric resonator ER 4118 SPT-NI. The temperature was varied in the range from 340 to 50 K ($\pm$1 K) by an Oxford instrument autotuning temperature controller. The EPR powder spectra were analyzed using the Bruker programs WINEPR to extract the basic spectral parameters and XSophe for simulation and fitting of spectra with anisotropic *g* factors and dipolar coupling tensor, **D**. Simulated separated doublet and triplet spectra were added together using simple routine in MATLAB. The triplet state is described by a dipolar coupling tensor, **D**, that can be parametrized in terms of two zero-field-splitting parameters (ZFS), *D* and *E*. The magnitude of $|D|$ is a measure of the delocalization of the molecular orbitals involved in the triplet state and is inversely proportional to the cube of the distance between the unpaired electrons. The magnitude of the second ZFS parameter $|E|$ is attributed to the extent of distortion from axial symmetry and lies in the range of $0 \leq 3|E|/|D| \leq 1$, where the extremes represent the axial ($|E| = 0$) and rhombic limit ($3|E|/|D| = 1$).

Variable-temperature magnetic susceptibility data were obtained using a Quantum Design MPMS5S SQUID magnetometer employing a magnetic field of 1000 Oe (numerical data are given in Table S1 in the Supporting Information). The air-sensitive compounds were contained in polycarbonate capsules. The molar magnetic moments were obtained by subtraction of the diamagnetic contribution of the capsules and sample holders, measured separately, from the experimental data sets. Background corrections for underlying diamagnetism (Pascal constants) were applied.

Elemental analyses were obtained from Galbraith Laboratories, Inc., Knoxville, Tennessee.

2.3. Computational Details. The molecular geometry optimizations, vibrational frequencies, and NBO charge calculations of $\mathbf{1}^{2+}$–$\mathbf{3}^{2+}$ were performed at the MPW1PW91[12a] level of theory. Potential energy scan calculations of radical pairs were performed with the CASSCF[12b–d] method, employing the 6-31G* basis set, as implemented into Gaussian03W suite of programmes.[13]

Single-point energy calculations of the broken-symmetry[14] state of dimers were carried out at the MPW1PW91/6-31G* level of theory (keyword *guess=mix*), with normal self-consistent field calculation criteria. Single-point energy calculations of the singlet–triplet gaps for isolated molecules $\mathbf{1}^{2+}$–$\mathbf{3}^{2+}$ were performed on the same level but with tight self-consistent field calculation criteria and fine integration grids.

All the calculated structures were visualized with ChemCraft.[15a]

2.4. Syntheses. 2.4.1. Preparation of 1[AsF_6]$_2$. $C_2F_4(CN)_2$ (0.115 g, 7.57×10^{-4} mol) was condensed into one bulb of a two-bulb vessel and dissolved in 11.3 g of SO_2. The solution was transferred into the second bulb containing a 1:1 mixture of $S_4(AsF_6)_2$ and $S_8(AsF_6)_2$, "S_3AsF_6" (0.430 g, 1.51×10^{-3} mol). After 2 days, red-brown crystals of sparingly soluble $C_2F_4(CNSSS)_2(AsF_6)_2$ were formed (0.393 g, 72% isolated yield). Elemental analysis for $C_4As_2F_{16}N_2S_6$, found/calcd (%): C, 6.36/6.65; N, 3.59/3.88. IR (cm^{-1}): 1540 vw, 1204 s, 1190 s, 1058 ms, 1020 vw, 861 m, 769 ms, 699 vs ($\nu_3 AsF_6^-$),[15b] 678 s (ν_1 AsF_6^-), 639 m, 585 w, 576 w (ν_2 AsF_6^-), 535 vw, 504 mw, 450 w, 395 vs (ν_4 AsF_6^-).

2.4.2. Preparation of 2[AsF_6]$_2$. $C_4F_8(CN)_2$ (0.140 g, 5.55×10^{-4} mol) was condensed into one bulb of a two-bulb vessel and was dissolved in 6.7 g of SO_2. The solution was transferred into the second bulb containing a 1:1 mixture of $S_4(AsF_6)_2$ and $S_8(AsF_6)_2$, "S_3AsF_6" (0.292 g, 1.02×10^{-3} mol). After 2 days, red-brown crystals of sparingly soluble $C_4F_8(CNSSS)_2(AsF_6)_2$ were formed (0.345 g, 76% isolated yield). Elemental analysis for $C_6As_2F_{20}N_2S_6$, found/calcd (%): C, 8.93/8.76; N, 3.25/3.41. IR (cm^{-1}): 1538 w, 1230 vs, 1202 vs, 1178 s, 1138 vs, 965 mw, 854 m, 712 vs, 690 vs (ν_3 AsF_6^-),[15b] 674 s (ν_1 AsF_6^-), 652 ms, 626 s, 582 vw, 564 m (ν_2 AsF_6^-), 535 mw, 524 vw, 506 m, 449 vw, 397 vs (ν_4 AsF_6^-).

2.4.3. Preparation of NCC_3F_6CN. $H_5C_2OOCC_3F_6COOC_2H_5$ (10 g, 0.034 mol) was placed in a 250 mL three-neck round-bottom flask and dissolved in 100 mL of dry Et_2O. Ammonia was bubbled through the solution with stirring. After 12 h, an insoluble white precipitate of $H_2NOCC_3F_6CONH_2$ was filtered off and dried under vacuum for several hours yielding 6.5 g (80%) of the product. The amide was thoroughly mixed with powdered P_2O_5 (30 g, ~4 fold excess) and placed in a 500 mL round-bottom flask. The system was attached to a vacuum line, evacuated, and heated at 150–200 °C for 30 min, while the collection bulb, attached to another end of the vacuum system, was held at −70 °C. The collected dinitrile (0.95 g, 16%) was purified by multiple vacuum distillations with a temperature gradient of 30–40 °C. The gas-phase IR spectrum contained a strong band at 2260 cm^{-1} and other stretches consistent with $C_3F_6(CN)_2$ structure. No bands attributable to C=O were observed. The dinitrile was used in the reaction immediately because of slow polymerization at room temperature.

2.4.4. Preparation of 3[AsF_6]$_2$·SO_2. $C_3F_6(CN)_2$ (0.259 g, 1.28×10^{-3} mol) was condensed into one bulb of a two-bulb vessel and dissolved in 15.7 g of SO_2. The solution was transferred into the second bulb containing a 1:1 mixture of $S_4(AsF_6)_2$ and $S_8(AsF_6)_2$, "S_3AsF_6" (0.631 g, 2.22×10^{-3} mol). After 3 days, a brown-orange solution was formed. The solvent was slowly evaporated until red-brown crystals of sparingly soluble C_3F_6-

(11) (a) Gillespie, R. J.; Passmore, J.; Ummat, P. K.; Vaidya, O. C. *Inorg. Chem.* **1971**, *10*, 1327. (b). Murchie, M. P.; Kapoor, R.; Passmore, J.; Schatte, G. *Inorg. Synth.* **1996**, *31*, 80.

(12) (a) Adamo, C.; Barone, V. *J. Chem. Phys.* **1998**, *108*, 664. (b) Werner, H.-J.; Knowles, P. J. *J. Chem. Phys.* **1985**, *82*, 5053. (c) Knowles, P. J.; Werner, H.-J. *Chem. Phys. Lett.* **1985**, *115*, 259. (d) Busch, T.; Degli Esposti, A.; Werner, H.-J. *J. Chem. Phys.* **1991**, *94*, 6708.

(13) Frisch, M. J.; Trucks, G. W.; Schlegel, H. B.; Scuseria, G. E.; Robb, M. A.; Cheeseman, J. R.; Montgomery, J. A., Jr.; Vreven, T.; Kudin, K. N.; Burant, J. C.; Millam, J. M.; Iyengar, S. S.; Tomasi, J.; Barone, V.; Mennucci, B.; Cossi, M.; Scalmani, G.; Rega, N.; Petersson, G. A.; Nakatsuji, H.; Hada, M.; Ehara, M.; Toyota, K.; Fukuda, R.; Hasegawa, J.; Ishida, M.; Nakajima, T.; Honda, Y.; Kitao, O.; Nakai, H.; Klene, M.; Li, X.; Knox, J. E.; Hratchian, H. P.; Cross, J. B.; Bakken, V.; Adamo, C.; Jaramillo, J.; Gomperts, R.; Stratmann, R. E.; Yazyev, O.; Austin, A. J.; Cammi, R.; Pomelli, C.; Ochterski, J. W.; Ayala, P. Y.; Morokuma, K.; Voth, G. A.; Salvador, P.; Dannenberg, J. J.; Zakrzewski, V. G.; Dapprich, S.; Daniels, A. D.; Strain, M. C.; Farkas, O.; Malick, D. K.; Rabuck, A. D.; Raghavachari, K.; Foresman, J. B.; Ortiz, J. V.; Cui, Q.; Baboul, A. G.; Clifford, S.; Cioslowski, J.; Stefanov, B. B.; Liu, G.; Liashenko, A.; Piskorz, P.; Komaromi, I.; Martin, R. L.; Fox, D. J.; Keith, T.; Al-Laham, M. A.; Peng, C. Y.; Nanayakkara, A.; Challacombe, M.; Gill, P. M. W.; Johnson, B.; Chen, W.; Wong, M. W.; Gonzalez, C.; and Pople, J. A.; *Gaussian 03*, revision C.02; Gaussian, Inc.: Wallingford, CT, 2004.

(14) (a) Noodleman, L.; Norman, J. G. *J. Chem. Phys.* **1979**, *70*, 4903. (b) Noodleman, L. *J. Chem. Phys.* **1981**, *74*, 5737.

(15) (a) Zhurko, D. A.; Zhurko, G. A. *ChemCraft 1.5*; Plimus: San Diego, CA, 92130; http://www.chemcraftprog.com (accessed Dec 2006). (b) Nakamoto, K. *Infrared and Raman Spectra of Inorganic and Coordination Compounds*; Wiley: New York, 1986. (c) Murchie, P. M.; Passmore, J.; Sutherland, G. W.; Kapoor, R. *J. Chem. Soc., Dalton Trans.* **1992**, 503.

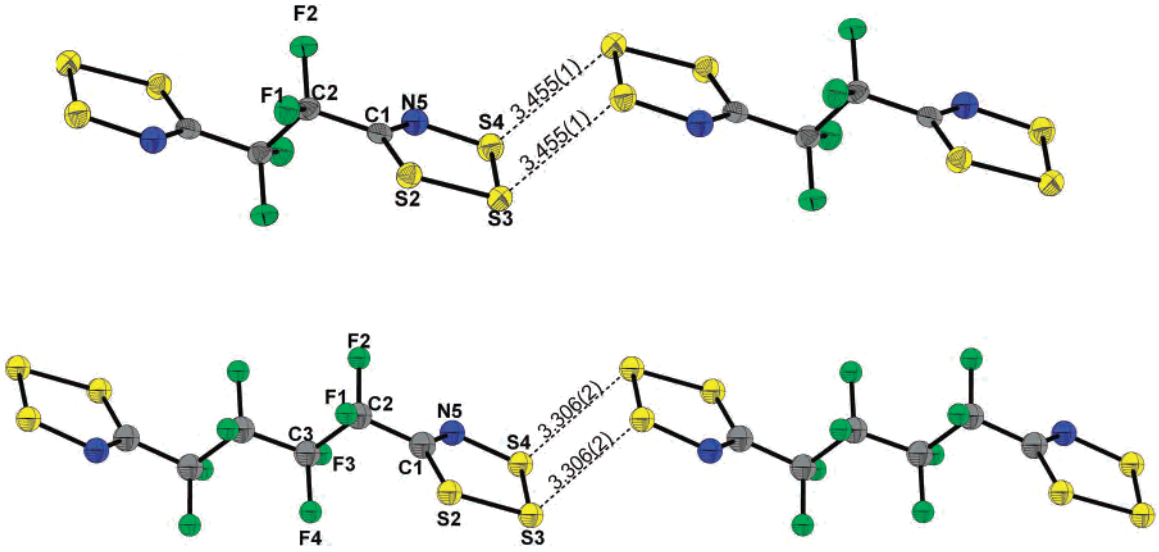

Figure 1. Dimers of dications of $\mathbf{1}^{2+}$ (top) and $\mathbf{2}^{2+}$ (bottom). Structural data are compiled in Table 1.

$(CNSSS)_2(AsF_6)_2 \cdot SO_2$ precipitated, which then were washed a few times with a small amount of SO_2 to afford 0.642 g of the product (65% isolated yield). Elemental analysis for $C_5As_2F_{18}N_2S_7O_2$, found/calcd (%): C, 9.15/7.18; N, 4.28/3.35. IR (cm^{-1}): 1543 w, 1331 s (ν_3 SO_2),[15c] 1288 s, 1231 s, 1193 vs, 1176 vs, 1148 m, 1109 s, 1008 mw, 965 w, 933 w, 885 m, 856 m, 785 m, 751 vs, 703 vs (ν_3 AsF_6^-), 675 vs (ν_1 AsF_6^-), 639 ms, 612 m, 582 w, 565 w (ν_2 AsF_6^-), 539 w, 523 w, 508 mw, 478 vw, 394 vs (ν_4 AsF_6^-).

EPR of dilute solutions of $\mathbf{1}[AsF_6]_2$, $\mathbf{2}[AsF_6]_2$, and $\mathbf{3}[AsF_6]_2 \cdot SO_2$ gave one resonance line at $g = 2.016(1)$, identical (within experimental error) to that of other $RCNSSS^{\bullet +}$ derivatives.[8−10]

The actual IR spectra of compounds with tentative frequency assignments are given in the Supporting Information.

2.5. X-ray Crystal Structure Determination. Crystal data for $\mathbf{1}[AsF_6]_2$: $C_4As_2F_{16}N_2S_6$, $M = 722.26$, crystal dimensions 0.40 × 0.20 × 0.05 mm^3, red plate, triclinic, space group $P\bar{1}$, $a = 6.5314(7)$ Å, $b = 7.5658(9)$ Å, $c = 9.6048(11)$ Å, $\alpha = 100.962(2)°$, $\beta = 96.885(2)°$, $\gamma = 107.436(2)°$, $V = 436.56(9)$ $Å^3$, $T = 173$ K, $Z = 1$, 2195 reflections collected, 1421 unique ($R_{int} = 0.0176$), R1 = 0.0412, wR2 = 0.1146 refined on F^2. Crystal data for $\mathbf{2}[AsF_6]_2$: $C_6As_2F_{20}N_2S_6$, $M = 822.28$, crystal dimensions 0.25 × 0.075 × 0.01 mm^3, red plate, monoclinic, space group $P2_1/c$, $a = 10.6398(16)$ Å, $b = 7.9680(11)$ Å, $c = 12.7468(19)$ Å, $\alpha = 90°$, $\beta = 99.758(2)°$, $\gamma = 90°$, $V = 1065.0(3)$ $Å^3$, $T = 173$ K, $Z = 2$, 7120 reflections collected, 2392 unique ($R_{int} = 0.0386$), R1 = 0.0389, wR2 = 0.0874 refined on F^2. Preliminary crystal data were obtained for $\mathbf{3}[AsF_6]_2 \cdot SO_2$: $C_5As_2F_{18}N_2S_7O_2$, $M = 836.27$, crystal dimensions 0.05 × 0.30 × 0.40 mm^3, red plate, triclinic, space group $P\bar{1}$, $a = 13.396(1)$ Å, $b = 13.333(1)$ Å, $c = 19.443(2)$ Å, $\alpha = 73.907(7)°$, $\beta = 86.359(5)°$, $\gamma = 87.602(6)°$, $V = 3329.0(5)$ $Å^3$, $T = 173$ K, $Z = 3$. There are six independent AsF_6^- anions; two are disordered over two positions each. Not all F atoms were found in Fourier difference maps. The quality of the crystal data was low because of the three SO_2 molecules present with partial occupancies, overlapping with the disordered AsF_6^- anions. This disorder could not be properly modeled.

All measurements were made on a Bruker AXS P4/SMART 1000 diffractometer with graphite-monochromated Mo Kα radiation. The structures were solved by direct methods,[16] and all atoms were refined anisotropically.

(16) Sheldrick, G. M. *SHELXS-97, Program for the Refinement of Crystal Structures*; University of Göttingen: Göttingen, Germany, 1997.

Table 1. Experimental (X-ray)[a] and Calculated (MPW1PW91/6-31G*) Bond Distances (Å) and Angles (deg) of $\mathbf{1}^{2+}$ and $\mathbf{2}^{2+}$ [b]

	$\mathbf{1}^{2+}$		$\mathbf{2}^{2+}$	
	X-ray	calcd	X-ray	calcd
C1−N5	1.266(6)	1.275	1.298(6)	1.275
C1−S2	1.742(5)	1.765	1.741(4)	1.765
N5−S4	1.607(4)	1.614	1.640(4)	1.614
S2−S3	2.019(2)	2.036	2.022(2)	2.036
S3−S4	2.069(2)	2.115	2.074(2)	2.115
C1−C2	1.525(7)	1.531	1.536(6)	1.535
C2−F1	1.329(6)	1.345	1.340(5)	1.348
C2−F2	1.334(5)	1.334	1.337(4)	1.334
C2−C2	1.558(6)	1.556		
C2−C3			1.557(5)	1.557
C3−F3			1.327(5)	1.338
C3−F4			1.351(4)	1.344
C3−C3			1.536(6)	1.558
S2−F1	2.778(3)	2.745	2.819(3)	2.722
C2−C1−S2	116.0(3)	116.1	116.3(3)	115.7
C1−S2−S3	97.0(2)	97.0	97.2(1)	97.1
S2−S3−S4	97.05(7)	97.2	97.6(7)	97.1
S3−S4−N5	100.9(2)	99.9	101.7(1)	99.9
C1−N5−S4	121.3(3)	122.8	118.8(4)	122.8
C2−C1−N5	120.5(4)	120.8	118.9(4)	121.3
F1−C2−C1−S2	15.4(5)	8.5	23.0(4)	9.2

[a] Numbering schemes are shown in Figure 1. [b] For $\mathbf{2}^{2+}$, mean internal parameters of the two molecular halves are given.

3. Results and Discussion

3.1. Syntheses of $\mathbf{1}[AsF_6]_2$, $\mathbf{2}[AsF_6]_2$, and $\mathbf{3}[AsF_6]_2 \cdot SO_2$. Preparation of $\mathbf{1}[AsF_6]_2$, $\mathbf{2}[AsF_6]_2$, and $\mathbf{3}[AsF_6]_2 \cdot SO_2$ was carried out analogously to the other previously known $RCNSSS^{\bullet +}$ derivatives (Scheme 1).[8−10] The high ionization potentials (IPs) of $C_xF_{2x}(CN)_2$ allowed us to carry out all the reactions by direct mixing of the two reagents, with no formation of byproducts.[9d] Large crystals of $\mathbf{1}[AsF_6]_2$, $\mathbf{2}[AsF_6]_2$, and $\mathbf{3}[AsF_6]_2 \cdot SO_2$ (appeared to be of uniform composition as examined under microscope) were prepared with isolated yields ranging from 65 to 76%. Satisfactory elemental analyses were obtained for $\mathbf{1}[AsF_6]_2$ and $\mathbf{2}[AsF_6]_2$. The elemental analysis of $\mathbf{3}[AsF_6]_2 \cdot SO_2$ indicated presence of minor quantities of unidentified impurities. IR spectra of all three compounds were consistent with the given formula-

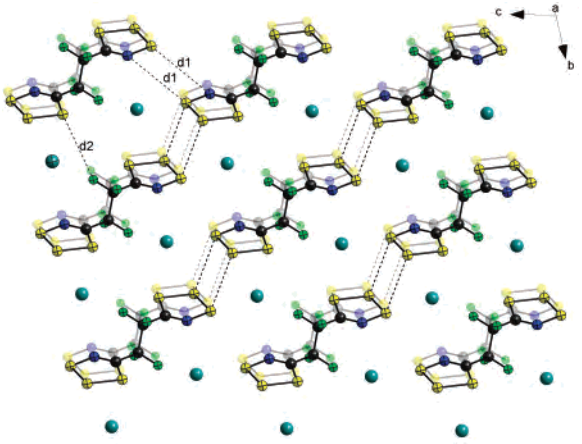

Figure 2. Projection of the unit cell of **1**$[AsF_6]_2$ onto the *bc* plane with the dimensions $2 \times a$, $3 \times b$, and $3 \times c$ (next layer of dications translated down the *a*-axis is faded for clarity). The AsF_6^- anions are represented by the single As atom for clarity. Selected intralayer S···N and S···F linkages (Å): $d_1 = 4.099(4)$, $d_2 = 3.965(3)$.

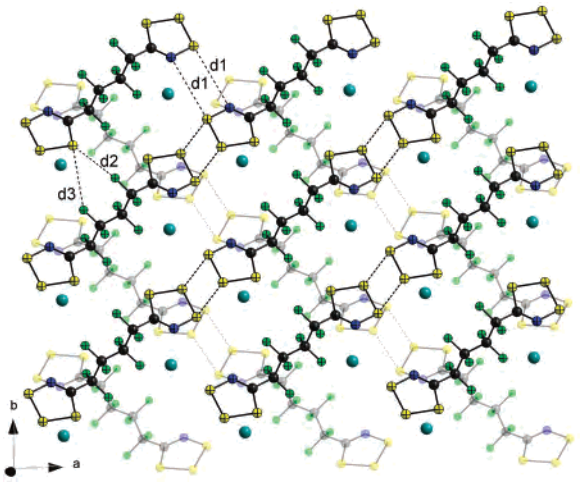

Figure 3. Projection of the unit cell of **2**$[AsF_6]_2$ onto the *ab* plane with the dimensions $2 \times a$, $3 \times b$, and $3 \times c$ (next layer of dications translated down the *c*-axis is faded for clarity). The AsF_6^- anions are represented by the single As atom for clarity. Selected intralayer S···N and S···F linkages (Å): $d_1 = 4.203(4)$, $d_2 = 3.335(3)$, $d_3 = 4.109(3)$.

tions, and the IR spectrum of **3**$[AsF_6]_2 \cdot SO_2$ contained a peak at 1331 cm^{-1} assignable to $\nu_3 SO_2$ (see Supporting Information, Table S2), indicating that the ground material still retained solvent molecules.

Scheme 1

$$C_xF_{2x}(CN)_2 + {}^1/_2S_8(AsF_6)_2 + {}^1/_2S_4(AsF_6)_2 \xrightarrow{SO_2} C_xF_{2x}(CNSSS^{\bullet+})_2(AsF_6^-)_2$$

$x = 2$, **1**$[AsF_6]_2$; $x = 4$, **2**$[AsF_6]_2$; $x = 3$, **3**$[AsF_6]_2 \cdot SO_2$

3.2. Solid-State Structures and Magnetic Properties of 1[AsF$_6$]$_2$ and 2[AsF$_6$]$_2$ and Magnetic Properties of 3[AsF$_6$]$_2$·SO$_2$. 3.2.1. Crystal Structures of 1[AsF$_6$]$_2$ and 2[AsF$_6$]$_2$. Two interacting dications $\mathbf{1}^{2+}$ and $\mathbf{2}^{2+}$ are illustrated in Figure 1. The experimental and calculated internal parameters of the isolated diradicals are compiled in Table 1 and appear to be similar to those found for other $RCNSSS^{\bullet+}$ rings.[8−10] The AsF_6^- anions possess distorted O_h geometry (Figure S1 in the Supporting Information).

In the solid-state, both **1**$[AsF_6]_2$ and **2**$[AsF_6]_2$ contain dications linked via weak four-centered two-electron $\pi^*-\pi^*$ bonds in a chainlike fashion (Figures 2 and 3). This gives a polymeric array of dications, but the dimeric interactions should be considered to be *local* because the dimeric pairs are isolated from each other by chains of carbons with sp^3 hybridization. The radicals associate via weak four-centered two-electron $\pi^*-\pi^*$ bonds in a *trans*-antarafacial fashion with S···S interactions of 3.455(1) {**1**$[AsF_6]_2$} and 3.306(2) Å {**2**$[AsF_6]_2$} (Figure 1). The same mode of association was found for $RCNSSS^{\bullet+}$ (R = Cl, Br, I),[8a] $[S_3N_2]_2^{2+}$,[17] and related $-CNSSN^{\bullet}$ ring systems,[18] with the longest S···S contact of 3.443(2) Å observed for sterically encumbered 2,4,6-$(F_3C)_3C_6H_2CNSSN^{\bullet}$[18c] {for most of the $[RCNSSN]_2$ dimers the intradimeric S···S distance falls in the range of 2.9−3.1 Å}.[1] We believe that the considerable difference in the length of intradimeric S···S interactions (~0.15 Å) for **1**$[AsF_6]_2$ and **2**$[AsF_6]_2$ stems from different packing motifs (see below) because the electronic properties of the $-CNSSS^{\bullet+}$ rings (e.g., charges and spin densities, Table 4 and section 3.3.1) are barely affected by a substituent group, similar to the previously reported $RCNSSS^{\bullet+}$ radical cations.[8c] Chains in both **1**$[AsF_6]_2$ and **2**$[AsF_6]_2$ form layers interleaved by AsF_6^- anions (Figures 2 and 3). However, some differences between these packing motifs can be noted. The major difference is that chains of $\mathbf{1}^{2+}$ propagate parallel with respect to the chains in neighboring layers, while chains of $\mathbf{2}^{2+}$ in adjacent layers are almost perpendicular to one another. We can speculate that the larger size of the dications $\mathbf{2}^{2+}$ makes it more difficult to pack in such a compact and symmetric pattern as observed in the structure of the smaller $\mathbf{1}^{2+}$ (cf., their densities of 2.564 Mg/m^3 and 2.747 Mg/m^3, respectively). At present, it is not clear how these slight changes in packing motifs reflect in the length of intradimeric S···S distances, leading to the shorter S···S contacts in **2**$[AsF_6]_2$. Unfortunately, structural exploration of diradicals $C_xF_{2x}(CNSSS)_2^{\bullet\bullet 2+}$ with $x > 4$ was limited because of their low crystallinity, perhaps as a result of larger chain size. Below we demonstrate how the minor changes in packing motifs of **1**$[AsF_6]_2$ and **2**$[AsF_6]_2$ affect magnetic and EPR properties of both salts, particularly reflecting in the strength of *inter*dicationic exchange interaction.

(17) (a) Banister, A. J.; Clarke, H. G.; Rayment, I.; Shearer, H. M. M. *Inorg. Nucl. Chem. Lett.* **1974**, *10*, 647. (b) Gillespie, R. J.; Ireland, P. R.; Vekris, J. E. *Can J. Chem.* **1975**, *53*, 3147. (c) Gillespie, R. J.; Kent, J. P.; Sawyer, J. F. *Inorg. Chem.* **1981**, *20*, 3784.

(18) (a) Cordes, A. W.; Haddon, R. C.; Hicks, R. G.; Oakley, R. T.; Palstra, T. T. M. *Inorg. Chem.* **1992**, *31*, 1802. (b) Britten, J. F.; Cordes, A. W.; Haddon, R. C.; Itkis, M. E.; Oakley, R. T.; Reed, R. W.; Robertson, C. M. *CrystEngComm.* **2002**, *4*, 205. (c) Alberola, A.; Clarke, C. S.; Haynes, D. A.; Pascu, S. I.; Rawson, J. M. *Chem. Commun.* **2005**, 4726. The β-phase of this compound in fact contains trimers.

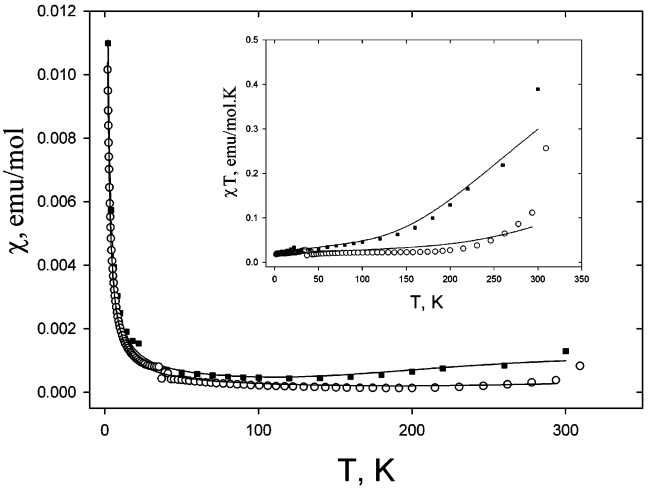

Figure 4. Temperature dependence of magnetic susceptibility for **1**$[AsF_6]_2$ (■) and **2**$[AsF_6]_2$ (○) (inset depicts the corresponding χT vs T plots). Solid lines represent fits to Bleaney−Bowers[19] model with the parameters given in the text and Table 2.

Table 2. Summary of the Parameters Extracted from Magnetic Data of **1**$[AsF_6]_2$ and **2**$[AsF_6]_2$

	model used	temp range (K)	$2J$ (cm^{-1})	ρ	TIP
1$[AsF_6]_2$	Bleaney−Bowers[19]	2−300	-500 ± 30	0.0284(3)	0.0002
2$[AsF_6]_2$	Bleaney−Bowers[19]	2−300	-900 ± 90	0.0245(1)	0.0001

3.2.2. Magnetic Properties of 1$[AsF_6]_2$ and 2$[AsF_6]_2$. Plots of χ versus T and χT versus T (insets) for the title salts are shown in Figure 4. The susceptibilities of both **1**$[AsF_6]_2$ and **2**$[AsF_6]_2$ are dominated by paramagnetic $1/T$ contributions at low temperatures and by gradual increases as the temperature rises above 150 K. Examination of the χT products (insets) shows the low-temperature products to be very small (∼0.02 emu K mol^{-1}), far below the expected value of 0.75 emu K mol^{-1} for an ideal diradical with noninteracting spins. The χT products increase with temperature, rapidly for **1**$[AsF_6]_2$ (∼0.4 emu K mol^{-1} at 300 K) and less rapidly for **2**$[AsF_6]_2$ (∼0.25 emu K mol^{-1} at 300 K). This behavior is consistent with the presence of strongly antiferromagnetically coupled dimers plus a few percent of paramagnetic monomers (Table 2). The data are in good agreement with the predictions of the Bleaney−Bowers model[19] with singlet−triplet gaps of -500 ± 30 and -900 ± 90 cm^{-1} for **1**$[AsF_6]_2$ and **2**$[AsF_6]_2$, respectively. The larger absolute value of the exchange interaction in **2**$[AsF_6]_2$ correlates with its shorter observed S···S contacts in the crystal structure {3.306(2) Å as opposed to 3.455(1) Å in **1**$[AsF_6]_2$}. This trend is also supported by the results of quantum chemical calculations (section 3.3.3).

In the previously described $[ClCNSSS]_2^{2+}$, the intradimeric distances were found to be even shorter [3.167(2) Å], further increasing the singlet−triplet gap to -1900 ± 100 cm^{-1}.[8a] Until this work, the latter value was the only experimental exchange interaction determined for any thiazyl radical dimer in the solid state. Current work allowed us to extend the number of such examples to three. As can be seen from the inset of Figure 4, at RT, **1**$[AsF_6]_2$ and **2**$[AsF_6]_2$ have significant χT values of ∼0.4 and 0.25 emu K mol^{-1}, respectively ($C = 0.75$ emu K mol^{-1} for two noninteracting unpaired spins). Although these values do not have real physical meaning in terms of a number of unpaired electrons per molecule, they indicate a substantial onset of paramagnetism in **1**$[AsF_6]_2$ and **2**$[AsF_6]_2$, which cannot be regarded as conventional diamagnetic materials. Related $\pi^*-\pi^*$ dimers of thiazyl radicals with shorter S···S interradical distances, that is, $[S_3N_2]_2^{2+}$ [17] and numerous derivatives of the RCNSSN• ring system,[1] have been regarded as diamagnetic materials, although we note that $[S_3N_2]_2[AsF_6]_2$ and the related $[I_2]_2[AsF_6]_2$ have been reported to have small residual paramagnetism.[20]

3.2.3. Solid-State EPR of 1$[AsF_6]_2$ and 2$[AsF_6]_2$. Since the geometry of the interdicationic four-centered two-electron $\pi^*-\pi^*$ interactions in the structures of **1**$[AsF_6]_2$ and **2**$[AsF_6]_2$ is essentially the same as that of $[ClCNSSS]_2^{2+}$, only with slightly longer S···S contacts, we expected the presence of triplet excitons in the title compounds at RT because thermal occupation of the triplet state at RT has already been detected for $[ClCNSSS]_2^{2+}$ (properties described in ref 8a). However, triplet signals were not observed in the RT EPR spectra of solid **1**$[AsF_6]_2$ or **2**$[AsF_6]_2$, although an intense spin-doublet spectrum was observed with anisotropic g values of 2.016, 2.025, and 2.001, which are characteristic of isolated thiazyl radicals. An intense spin-doublet signal, with the g factors identical to those of the $S = 1$ state, was also present in the EPR spectrum of $[ClCNSSS]_2^{2+}$. This intrinsic signal was assigned to defect lattice sites, that is, sites missing half of the radical pair, and we assign this signal in **1**$[AsF_6]_2$ and **2**$[AsF_6]_2$ similarly (see below).

However, when cooled to a temperature below ∼280 K, a characteristic triplet spectrum was observed for **2**$[AsF_6]_2$, including the "forbidden" half-field transition (Figure 5A). The lack of resolution of this spectrum at RT likely arises from broadening of the resonance lines. The zero-field-splitting (ZFS) parameters were extracted by simulation of the 230 K spectrum. Given the very similar structural features of the intercationic interaction in **2**$[AsF_6]_2$ and $[ClCNSSS]_2^{2+}$, it seemed likely that there would be significant non-coincidence between the g matrix and the D tensor axes for **2**$[AsF_6]_2$, as found for $[ClCNSSS]_2^{2+}$.[8a] Specifically, we expected g_{zz} (∼g_e) to be perpendicular to the plane of the radical cations and D_{zz} to be oriented toward the interradical cationic separation. Given the very similar angles between the planes of the two radical cations and the interradical separation found for these two species, we attempted a simulation of the EPR spectrum of **2**$[AsF_6]_2$ using the same set of non-coincidence angles that we previously determined from a single-crystal EPR study of $[ClCNSSS]_2^{2+}$ and then made minor adjustments to the g and ZFS parameters. This gave a very good fit to the experimental spectrum (Figure 5A, Table 3). The temperature dependence of the (double

(19) Bleaney, B.; Bowers, K. D. *Proc. R. Soc. London* **1952**, *A214*, 451.

(20) The χT value of $[S_3N_2]_2[AsF_6]_2$ is 0.06 emu K mol^{-1} ($\mu_{eff} = 0.7$ μ_B; Kent, J. P. Ph.D. Thesis, McMaster University, Hamilton, Canada, 1984) and that of $[I_2]_2[AsF_6]_2$ equals 0.16 emu K mol^{-1} ($\mu_{eff} = 1.2$ μ_B; Murchie, M. P. Ph.D. Thesis, University of New Brunswick, Fredericton, Canada, 1986) at room temperature.

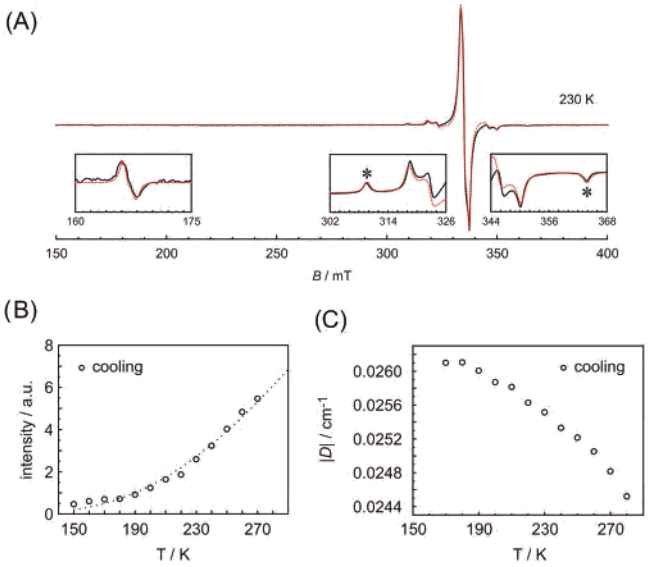

Figure 5. (A) EPR spectrum of a powder sample of **2**$[AsF_6]_2$ recorded at X-band at 230 K (solid black line) and its simulation (dotted red line). Insets show details of the ZFS structure of the $S = 1$ excited state. Simulation parameters are collected in Table 3. (B) The temperature dependence of the intensity of the triplet resonance lines marked by an asterisk (*) and fitted by the Bleaney−Bowers model[19] using the least-squares method (dotted line). (C) The temperature dependence of the ZFS parameter, $|D|$.

Table 3. Spin-Hamiltonian Parameters of the Paramagnetic Centers in the EPR Spectra of Solid **2**$[AsF_6]_2$

S	g_{xx}	g_{yy}	g_{zz}	$\|D\|$ (cm^{-1})	$\|E\|$ (cm^{-1})
1/2 doublet	2.016(1)	2.025(1)	2.001(1)		
1 triplet	2.016(1)	2.025(1)	2.001(1)	0.0254(8)	0.0013(8)
Euler angles transforming axis system of the g matrix to the axis system of the D tensor			$\alpha = 93°$	$\beta = 152°$	$\gamma = 139°$

integral) intensity of the $S = 1$ signal in the range of 150−280 K (Figure 5B) was fitted to the Bleaney−Bowers model[19] to give a singlet−triplet gap of -910 ± 70 cm^{-1}, in excellent agreement with the value obtained from the magnetic susceptibility measurements (-900 ± 90 cm^{-1}). We note that in both cases the Bleaney−Bowers model is not strictly obeyed because of a minor contraction of S···S contacts at lower temperatures, as was observed for the AsF_6^- salt of $[ClCNSSS]_2^{2+}$. In the latter dimer, ~0.1 Å shortening of the S···S distance occurred in the approximately 100 K temperature range (as determined by X-ray), accompanied by an increase in the magnitude of the D tensor from ~0.025 to 0.027 cm^{-1}.[8a] Since a similar increase in the magnitude of the D tensor occurs for **2**$[AsF_6]_2$ (from ~0.024 to 0.026 cm^{-1}, Figure 5C) one could expect a concomitant shortening of the intradimeric S···S contacts by about 0.1 Å. Hence the extracted singlet−triplet gap of **2**$[AsF_6]_2$, as well as that of **1**$[AsF_6]_2$, must be treated as average parameters. Using the value of -910 cm^{-1}, the percentage of molecules in triplet state in the solid **2**$[AsF_6]_2$ at RT was estimated to be 1.25%. This is much higher than that found for $[ClCNSSS]_2^{2+}$ at RT (which has a larger singlet−triplet gap), and we propose that this leads to broadening of the EPR resonance lines at RT caused by dipole−dipole interactions. Simulation of the entire 230 K spectrum of **2**$[AsF_6]_2$ gave the weighting of the triplet to doublet signals as 1:24. Given a singlet−triplet gap of -910 cm^{-1} and the population of the spin triplet state of 0.34%, we can calculate the percentage of lattice defect sites (leading to the spin-doublet spectrum) as ~4% at 230 K. A similar value of 2.45(1)% was obtained from magnetic susceptibility measurements (Table 2).

Table 4. Calculated Spin Densities and NBO Charges of $\mathbf{1}^{2+}$−$\mathbf{3}^{2+}$ Using the MPW1PW91/6-31G* Level of Theory[a]

	$\mathbf{1}^{2+}$		$\mathbf{2}^{2+}$		$\mathbf{3}^{2+}$	
	spin density	NBO charge	spin density	NBO charge	spin density	NBO charge
C1	−0.013184	−0.00669	−0.01616	0.00743	−0.017847	0.00541
C2	−0.001371	0.72471	−0.00252	0.71927	−0.002470	0.71960
C3			0.001413	0.68803	0.002549	0.69391
S2	0.283433	0.47468	0.283732	0.47012	0.283019	0.47491
S3	0.387473	0.25206	0.379319	0.23346	0.382861	0.24170
S4	0.314077	0.74069	0.316321	0.72843	0.316070	0.72891
N5	0.029475	−0.54348	0.037689	−0.54334	0.037065	−0.54851
F1	−0.000290	−0.32822	−0.000094	−0.33245	−0.000232	−0.33084
F2	0.000386	−0.31375	0.0002935	−0.30749	0.000386	−0.30518
F3			−0.000076	−0.32693	−0.000127	−0.33293
F4			0.0000845	−0.33653	−0.000127	−0.33293

[a] Atom labeling is given in Figure 1.

In contrast to **2**$[AsF_6]_2$, which clearly exhibited triplet species, we were unable to resolve allowed $\Delta M_s = \pm 1$ transitions in the solid-state X-band EPR spectrum of powdered **1**$[AsF_6]_2$ in the temperature range of 110−300 K. Some evidence for the presence of the triplet species arises from the S-band spectra in which a weak half-field transition was observed at low temperatures. This result (lack of observation of triplet species) may seem counterintuitive at first sight, given the fact that the dimeric pairs in solid **1**$[AsF_6]_2$ have longer S···S contacts and consequently a *smaller* singlet−triplet gap. From the Boltzmann relation, using the singlet−triplet gap determined from magnetic susceptibility data (-500 cm^{-1}), we calculated that 8.5% of radical pairs are in the triplet state at RT. Therefore, dipole−dipole interactions between triplets are much more pronounced in **1**$[AsF_6]_2$, leading to the collapse of the ZFS structure in the EPR spectrum because of line broadening effects. Similar effects were previously observed for a number of $[TCNQ^{\bullet -}]_2$ salts with moderate singlet−triplet gaps, and often, the dipolar components could only be resolved upon cooling to cryogenic temperatures (<20 K).[21]

3.2.4. Magnetic Properties of 3$[AsF_6]_2$·SO_2. Preliminary magnetic susceptibility measurements obtained on the polycrystalline sample of **3**$[AsF_6]_2$·SO_2 (Figure 6) indicated that it was paramagnetic in nature. The value of χT at RT (0.83 emu K mol^{-1}) was consistent with a molecule containing two noninteracting unpaired spins. Variable-temperature magnetic susceptibility measurements showed an interesting magnetic behavior with a steep decrease of magnetic susceptibility below 200 K, presumably indicative of a structural phase transition (Figure 6). However an extensive discussion of this phenomenon is only possible when definitive structural evidence on **3**$[AsF_6]_2$·SO_2 is obtained.

(21) Coulon, C.; Clerac, R. *Chem. Rev.* **2004**, *104*, 5655 and references therein.

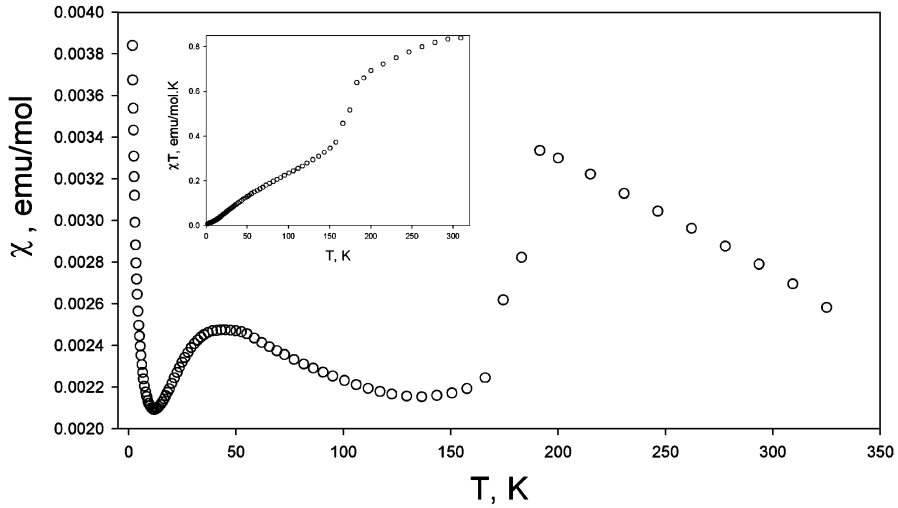

Figure 6. Temperature dependence of magnetic susceptibility for $\mathbf{3}[AsF_6]_2 \cdot SO_2$. The inset depicts the corresponding χT vs T plot.

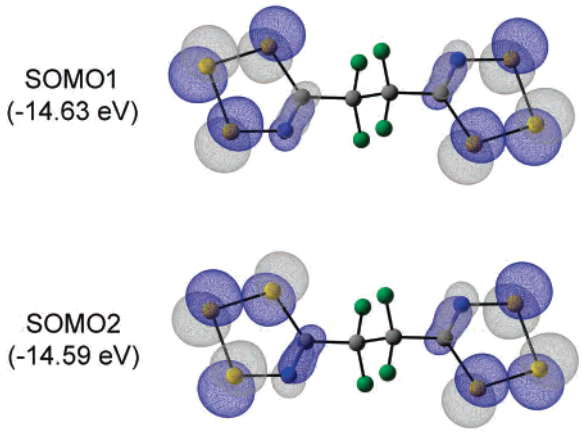

Figure 7. Diagram illustrating SOMOs of $\mathbf{1}^{2+}$ drawn at the isosurface of 0.04 au.

More detailed studies of the magnetic behavior of this compound are in progress (see Supporting Information).

3.3. Computational Analysis. 3.3.1. Calculated Structures of Isolated $\mathbf{1}^{2+}-\mathbf{3}^{2+}$. DFT-optimized molecular structures of $\mathbf{1}^{2+}$ and $\mathbf{2}^{2+}$ (bond lengths, angles, and dihedral angles) were rather similar to their X-ray geometries (see Table 1 and Figure S2 in the Supporting Information).[22]

Since molecules $\mathbf{1}^{2+}-\mathbf{3}^{2+}$ were explicitly designed to inhibit interaction between two radical centers, it is not surprising to find that the electronic properties of the two rings in $\mathbf{1}^{2+}-\mathbf{3}^{2+}$ are almost identical (Table 4). The two SOMOs of $\mathbf{1}^{2+}-\mathbf{3}^{2+}$ are essentially separated on the two heterocyclic rings (Figure 7, shown for the representative derivative $\mathbf{1}^{2+}$). With a broken-symmetry DFT approach, the calculated singlet−triplet gaps of *isolated* diradicals are +0.81, −0.18, and +0.13 cm^{-1} for $\mathbf{1}^{2+}$, $\mathbf{2}^{2+}$, and $\mathbf{3}^{2+}$, respectively. These numbers are very small and indicate negligible communication between unpaired electrons. Experimentally this is consistent with isotropic solution EPR spectra of $\mathbf{1}^{2+}-\mathbf{3}^{2+}$ containing one single line with $g = 2.016$-(1), typical of $RCNSSS^{\bullet+}$ monoradicals,[8−10] and showing no dipolar splittings. Therefore, isolated (as in the solution or gas phase) $\mathbf{1}^{2+}-\mathbf{3}^{2+}$ are, as expected, pure diradicals (100% diradical character). However, substantial *inter*molecular interaction experimentally observed for $\mathbf{1}[AsF_6]_2$ and $\mathbf{2}[AsF_6]_2$ in the solid state leads to one-dimensional polymers of $\mathbf{1}^{2+}$ and $\mathbf{2}^{2+}$ linked via weak four-centered two-electron $\pi^*-\pi^*$ bonds. This situation warrants more detailed analysis given below.

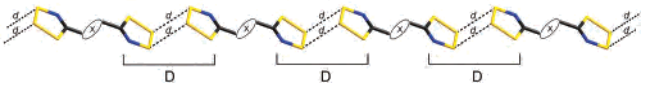

Figure 8. Schematic illustration of a polymeric array of D in the solids of $\mathbf{1}[AsF_6]_2$ [X = C_2F_4; d = 3.455(1) Å] and $\mathbf{2}[AsF_6]_2$ [X = C_4F_8; d = 3.306(2) Å]. D = four-centered two-electron $\pi^*-\pi^*$ bond.

3.3.2. Potential Energy Scan Calculations of $[ClCNSSS]_2^{2+}$. The polymeric arrays of dications interacting via four-centered two-electron $\pi^*-\pi^*$ bonds in the structures of $\mathbf{1}[AsF_6]_2$ and $\mathbf{2}[AsF_6]_2$ are graphically illustrated in Figure 8. The noninteracting nature of the SOMOs in $\mathbf{1}^{2+}$ and $\mathbf{2}^{2+}$ (Figure 7) allows us to describe the behavior of polymeric chains as that of isolated dimeric units, obeying a classical singlet−triplet model. Because of this fortunate circumstance, computational analysis can be restricted to the analysis of $RCNSSS^{\bullet+}$ radical pairs, with a Cl atom chosen as a substituent for simplicity. This then gives the $[ClCNSSS]_2^{2+}$ dimer, previously reported in a preliminary communication.[8a] It was already pointed out that the geometrical mode of association in the latter is essentially the same as that of $\mathbf{1}^{2+}$ and $\mathbf{2}^{2+}$. Thus, theoretical considerations applied to $[ClCNSSS]_2^{2+}$ are also suitable for radical pairs observed in the polymeric arrays of $\mathbf{1}^{2+}$ and $\mathbf{2}^{2+}$.

An inherent one-configurational nature of both broken-symmetry and closed-shell DFT algorithms makes them unsuitable to correctly describe the electronic states of the $[ClCNSSS]_2^{2+}$ dimer. Although in the previous work,[8a] we reported $[ClCNSSS]_2^{2+}$ to be metastable in the gas phase using the closed-shell $S = 0$ DFT method (MPW1PW91/6-31G*), the computed minimum could be an artifact, that is,

(22) Optimized geometry of $\mathbf{2}^{2+}$ imposed with C_i symmetry constraints (0° twist angle between two radical rings) was in fact a first-order saddle point. A minimum was found with C_1 symmetry (31° twist angle), and all the calculated parameters quoted in the text belong to this structure. Optimized geometries of $\mathbf{1}^{2+}$ and $\mathbf{3}^{2+}$ were of C_i and C_2 symmetries, respectively, and showed no imaginary frequencies.

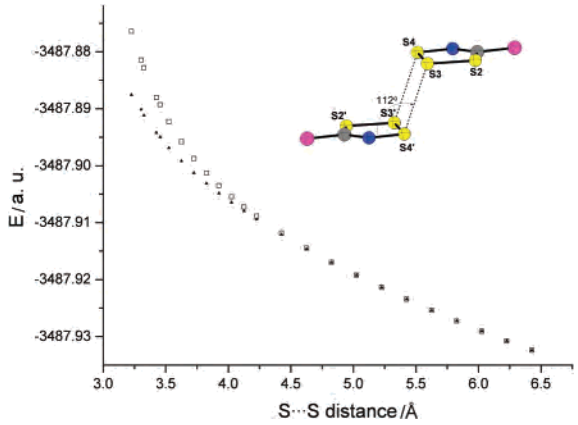

Figure 9. Calculated [CASSCF(6,6)/6-31G*] dependence of singlet (▲) and triplet (□) energies on the intradimeric S···S distance in the $[ClCNSSS]_2^{2+}$ dimer.

a consequence of the double-occupancy restriction to the orbitals imposed by any closed-shell method. The correct modeling of the overall wavefunction requires the use of *multiconfigurational* methods, such as CASSCF, that allows mixing-in of other wave functions from the orbitals of higher energy. In this work, we reconsidered the situation and performed a potential energy scan along the intradimeric S···S distance using the CASSCF(6,6)/6-31G* method, with calculation of both singlet and triplet states (Figure 9). The results indicate that the dimer at that level of theory has *no* minimum in either triplet or singlet spin states on the potential energy surface (along the interannular S···S coordinate), contrary to our previously reported results of closed-shell DFT calculations, where such a minimum was found. It is possible that higher-level calculations would show that there is an intrinsic minimum in the gas phase. Alternatively, it could be that the overall electrostatic interaction not only compensates for the repulsive energy between the positively charged rings in the dimer but also leads to the particular dimer geometry observed in the solid state. This arrangement featuring partially positively charged sulfur atoms, interacting via four-centered two-electron $\pi^*-\pi^*$ bonds, is very common, and we suspect that it possesses intrinsic stability. Most polyatomic doubly charged species are unstable in the gas phase with respect to dissociation into singly charged fragments.[23] The unfavorable dissociation energy is more than offset by the gain in lattice energy on formation of a 2:1 salt. For example, $S_3N_2(AsF_6)_2$ (s), containing $S_3N_2^{2+}$, is stable in the solid-state even though $S_3N_2^{2+}$ is unstable in the gas phase with respect to SN^+ and SNS^+.[23a] In the case of $[ClCNSSS]_2[AsF_6]_2$ (s), the repulsive energy of the $[ClCNSSS]_2^{2+}$ dimer in the gas phase is more than compensated by the overall lattice energy of the solid as a whole, including favorable electrostatic terms arising from cation−anion attraction, as well as repulsive terms between ions of like charge.

(23) (a) Brooks, W. V. F.; Cameron, T. S.; Parsons, S.; Passmore, J.; Schriver, M. J. *Inorg. Chem.* **1994**, *33*, 6230. (b) Krossing, I.; Passmore, J. *Inorg. Chem.* **1999**, *38*, 5203. (c) Cameron, T. S.; Dionne, I.; Jenkins, H. D. B.; Parsons, S.; Passmore, J.; Rowbottom, H. K. *Inorg. Chem.* **2000**, *39*, 2042. (d) Cameron, T. S.; Deeth, R. J.; Dionne, I.; Du, H.; Jenkins, H. D. B.; Krossing, I.; Passmore, J.; Roobottom, H. K. *Inorg. Chem.* **2000**, *39*, 5614.

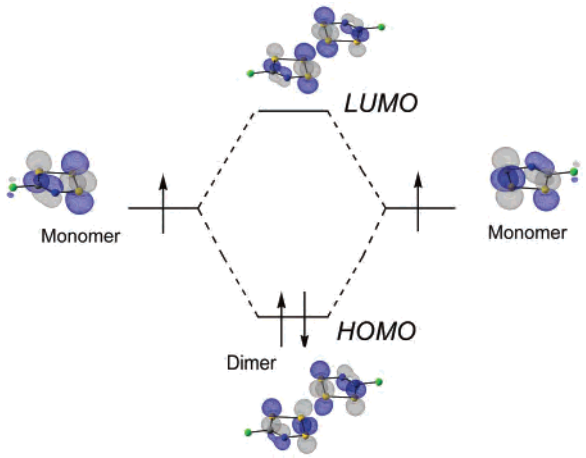

Figure 10. Schematic diagram illustrating formation of the $[ClCNSSS]_2^{2+}$ dimer from two monomers. Orbitals drawn at the isosurface of 0.05 au.

3.3.3. Calculation of Singlet−Triplet Gaps and Diradical Characters of the Four-Centered Two-Electron $\pi^*-\pi^*$ Bonds in Polymeric $\mathbf{1}^{2+}$ and $\mathbf{2}^{2+}$. Calculated singlet−triplet gaps of radical pairs in $[\mathbf{1}^{2+}]_n$ and $[\mathbf{2}^{2+}]_n$ can be obtained from Figure 9 using the S···S distances determined experimentally. Extrapolation of these values (3.455 and 3.303 Å, respectively) onto the *y*-axis gives the singlet−triplet gaps for the $\pi^*-\pi^*$ bonds in solid $\mathbf{1}[AsF_6]_2$ and $\mathbf{2}[AsF_6]_2$ as −1250 and −1900 cm^{-1}, respectively. The ratio of these two values (0.65) is in fairly good agreement with the ratio of the experimentally determined singlet−triplet gaps (0.56). We note that in both cases the calculated singlet−triplet gaps are approximately twice the experimental values extracted from the magnetic susceptibility data (see section 3.2.2).

As the two monomers are separated, the magnitude of antiferromagnetic exchange interaction decreases and approaches zero above 4.5 Å (Figure 9). Thus, beyond this benchmark the system can be considered as a pure diradical (∼100% diradical character), with the unpaired electrons occupying nearly degenerate MOs. Below 4.5 Å, a bonding interaction between two monoradicals arises causing the frontier orbitals to split into the bonding and antibonding combinations (Figure 10). Because of the somewhat long intermolecular S···S distances found in polymeric $[\mathbf{1}^{2+}]_n$ and $[\mathbf{2}^{2+}]_n$ [3.455(1) and 3.303(2) Å, respectively, cf., conventional S−S single bond of 2.06 Å], this splitting does not result in a double occupancy of HOMO as idealistically shown in Figure 10. We attempted to gain some insights into a nature of these weak four-centered $\pi^*-\pi^*$ bonds by computing natural orbital occupation numbers that have previously proven to be useful in the analysis of singlet diradical ground states.[24] Using a multiconfigurational CASSCF(6,6)/6-31G* method, we found that in radical pairs of $\mathbf{1}^{2+}$ and $\mathbf{2}^{2+}$ the LUMO occupation numbers equal 0.618 and 0.529, respectively. Approximately the same numbers were

(24) (a) Döhnert, D.; Koutecky, J. *J. Am. Chem. Soc.* **1980**, *102*, 1789. (b) Jung, Y.; Head-Gordon, M. *J. Phys. Chem. A* **2003**, *107*, 7475. (c) Jung, Y.; Head-Gordon, M. *Chem. Phys. Chem* **2003**, *4*, 522. (d) Aikens, C.; Gordon, M. S. *J. Phys. Chem. A* **2003**, *107*, 104. (e) Bendikov, M.; Duong, H. M.; Starkey, K.; Houk, K. N.; Carter, E. A.; Wudl, F. *J. Am. Chem. Soc.* **2004**, *126*, 7416.

systematically obtained on increase of the active space from (6,6) to (10,10). When the LUMO occupation numbers are divided by the corresponding HOMO occupation numbers (1.374 and 1.464, respectively), we can calculate that the $\pi^*-\pi^*$ bonds in polymeric chains of $\mathbf{1}^{2+}$ and $\mathbf{2}^{2+}$ possess diradical characters of 45 and 36%, respectively, assuming that the level of calculations is sufficiently high. An alternative description of a diradical character with Neese index,[25] using the broken-symmetry MPW1PW91/6-31G* method, gave somewhat higher values (60 and 50%; expectation values $<S^2>_{BS} = 0.84$ and 0.75, respectively). The four-centered $\pi^*-\pi^*$ bonds in the $[ClCNSSS]_2^{2+}$ dimer possess a similar diradical character (32% from natural orbital analysis and 37% from Neese index; $<S^2>_{BS} = 0.60$) calculated with the geometry fixed at the S···S distance of 3.167 Å.

The obtained values of diradical characters are intermediate between those of conventional closed-shell (~0) and open-shell (~100%) systems. In that respect, the $[ClCNSSS]_2^{2+}$ and the radical pairs observed in polymeric $[\mathbf{1}^{2+}]_n$ and $[\mathbf{2}^{2+}]_n$ may be regarded as diradicaloids. Intramolecular diradicaloid (diradical) behavior has been proposed in a number of heterocyclic ring systems and heavier alkyne congeners of current interest.[26]

We envision that other thiazyl radical dimers can be described in a similar way because they contain radical moieties linked by weak four-centered or multicentered two-electron $\pi^*-\pi^*$ bonds with the S···N and S···S contacts ranging from ~2.9 to 3.2 Å. These include $[S_3N_2]_2^{2+}$,[17] in which the dimerization mode is identical to that of $[ClCNSSS]_2^{2+}$, and numerous examples of $[RCNSSN]_2$[1] radical dimers with particularly long S···S distances in various association modes, as well as a few examples of $[RCSNSCR]_2$,[5b,7a,27] $[RCNSSCR']_2$,[28] and $[RCNSNSNR]_2$[29] thiazyl radical dimers.

We note that there are many organic radicals and radical ions that dimerize in the solid state through $\pi-\pi$ overlap between the SOMOs. For instance, recently, a thorough analysis of four-centered two-electron carbon−carbon bonds observed in the $[TCNE]_2$[2] dimer has been presented.[30] The other well-known examples of neutral radicals and radical ions forming dimeric pairs with multicentered π bonding include tris-*tert*-buthyl-phenalenyl,[31a] diazaphenalenyl,[31b] tetrathiafulvalenium, $TTF^{\bullet+}$,[32] terthiophenium[33a] and related π dimers,[33b] tetramethylphenylenediamonium, $TMPD^{\bullet+}$,[34] tetracyanoquinodimethanide $TCNQ^{\bullet-}$[21,35,36] and its tetrafluoro analog,[37] dichlorodicyanobenzoquinonide, $DDQ^{\bullet-}$,[38] and other quinoidal based radical anions.[39] In addition, there are a number of simple inorganic species, for example, $[I_2^+]_2$,[40a,b] S_8^{2+},[40c] $[SI_2^+]_2$,[40d] $[SeI_2^+]_2$,[41] $O_2Cl_2^+$,[40e] and $[NO]_2$,[40f] that can be viewed as being composed of two radical units linked by multicentered $\pi-\pi$ bonds. All these compounds therefore warrant relevant theoretical and experimental studies.

4. Conclusions

The $RCNSSS^{\bullet+}$ radical cations present an emerging class of nonsterically hindered stable radicals that are primarily sulfur based, with ~95% spin density residing on sulfur atoms and only ~5% on nitrogen. Thus, these radical cations are rare examples[42] of the heavier, non-second-row elements. In this article, we have explored the series of AsF_6^- salts of the dication diradicals of general formula $C_xF_{2x}(CNSSS)_2^{\bullet\bullet 2+}$ ($x = 2-4$) and described their physical properties as a function of spacer size, using X-ray, solid-state EPR, and

(25) Bachler, V.; Olbrich, G.; Neese, F.; Wieghardt, K. *Inorg. Chem.* **2002**, *41*, 4179. According to this index, the diradical character is calculated as $n = 100[1-(1-<S^2>_{BS})^{1/2}]$.

(26) (a) Niecke, E.; Fuchs, A.; Baumeister, F.; Nieger, M.; Schoeller, W. W. *Angew. Chem., Int. Ed. Engl.* **1995**, *34*, 555. (b) Scheschkewitz, D.; Amii, H.; Gornitzka, H.; Schoeller, W. W.; Bourissou, D.; Bertrand, G. *Science* **2002**, *295*, 1880. (c) Cui, C.; Brynda, M.; Olmstead, M. M.; Power, P. P. *J. Am. Chem. Soc.* **2004**, *126*, 6510. (d) Cox, H.; Hitchcock, P. B.; Lappert, M. F.; Pierssens, L. J.-M. *Angew. Chem., Int. Ed.* **2004**, *43*, 4500. (e) Jung, Y.; Brynda, M.; Power, P. P.; Head-Gordon, M. *J. Am. Chem. Soc.* **2006**, *128*, 7185.

(27) (a) Wolmershauser, G.; Kraft, G. *Chem. Ber.* **1989**, *122*, 385. (b) Wolmershauser, G.; Kraft, G. *Chem. Ber.* **1990**, *123*, 881.

(28) (a) Barclay, T. M.; Beer, L.; Cordes, A. W.; Oakley, R. T.; Preuss, K. E.; Taylor, N. J.; Reed, R. W. *Chem. Commun.* **1999**, 531. (b) Oakley, R. T.; Reed, R. W.; Robertson, C. M.; Richardson, J. F. *Inorg. Chem.* **2005**, *44*, 1837.

(29) (a) Boeré, R. T.; French, C. L.; Oakley, R. T.; Cordes, A. W.; Privett, J. A. J.; Craig, S. L.; Graham, J. B. *J. Am. Chem. Soc.* **1985**, *107*, 7710. (b) Boeré, R. T.; Fait, J.; Larsen, K.; Yip, J. *Inorg. Chem.* **1992**, *31*, 1417.

(30) (a) Miller, J. S.; Novoa, J. J. *Acc. Chem. Res.* **2007**, *40*, 189. (b) Del Sesto, E.; Miller, J. S.; Lafuente, P.; Novoa, J. J. *Chem.—Eur. J.* **2002**, *8*, 4894.

(31) (a) Goto, K.; Kubo, T.; Yamamoto, K.; Nakasuji, K.; Sato, K.; Shiomi, D.; Takui, T.; Kubota, M.; Kobayashi, T.; Yakushi, K.; Ouyang, J. J. Am. Chem. Soc. **1999**, *121*, 1619. (b) Morita, Y.; Aoki, T.; Fukui, K.; Nakazawa, S.; Tamaki, K.; Suzuki, S.; Fuyuhiro, A.; Yamamoto, K.; Sato, K.; Shiomi, D.; Naito, A.; Takui, T.; Nakasuji, K. *Angew. Chem., Int. Ed.* **2002**, *41*, 1793.

(32) Guirauden, A.; Johannsen, I.; Batail, P.; Coulon, C. *Inorg. Chem.* **1993**, *32*, 2446 and references therein.

(33) (a) Yamazaki, D.; Nishinaga, T.; Tanino, N.; Komatsu, K. *J. Am. Chem. Soc.* **2006**, *128*, 14470. (b) Miller, L. L.; Mann, K. R. *Acc. Chem. Res.* **1996**, *29*, 417.

(34) Hove, M. J.; Hoffman, B. M.; Ibers, J. A. *J. Chem. Phys.* **1972**, *56*, 3490.

(35) (a) Chesnut, D. B.; Arthur, P., Jr. *J. Chem. Phys.* **1962**, *36*, 2969. (b) Jones, M. T.; Chesnut, J. B. *J. Chem. Phys.* **1963**, *38*, 1311. (c) Bailey, J. C.; Chesnut, J. B. *J. Chem. Phys.* **1969**, *56*, 3490.

(36) (a) Hibma, T.; Sawatzky, G. A.; Kommandour, J. *Phys. Rev. B* **1977**, *15*, 3959. (b) Flandrois, S.; Choukroun, M. L.; Delhaes, P. *Mol. Cryst. Liq. Cryst.* **1979**, *52*, 35. (c) Reis, A. H., Jr.; Gebert, E.; Miller, J. S. *Inorg. Chem.* **1981**, *20*, 313. (d) Hoffmann, S. K.; Corvan, P. J.; Singh, P.; Sethulekshmi, C. N.; Metzger, R. M.; Hatfield, W. E. *J. Am. Chem. Soc.* **1983**, *105*, 4608. (e) Hynes, R. C.; Morton, J. R.; Preston, K. F.; Williams, A. J.; Evans, F.; Grossel, M. C.; Sutcliffe, L. H.; Weston, S. C. *J. Chem. Soc., Faraday Trans.* **1991**, *87*, 2229. (f) Grossel, M. C.; Weston, S. C. *Chem. Mater.* **1996**, *8*, 977.

(37) (a) Metzger, R. M.; Heimer, N. E.; Gundel, D.; Sixl, H.; Harms, R.; Keller, H. J.; Nöthe, D.; Wehe, D. *J. Chem. Phys.* **1982**, *77*, 6203. (b) Azcondo, T.; Ballester, L.; Golhen, S.; Gutierrez, A.; Ouahba, L.; Yartsev, S.; Delhaes, P. *J. Mater. Chem.* **1999**, *6*, 1237. (c) Johnson, M. T.; Arif, A. M.; Miller, J. S. *Eur. J. Inorg. Chem.* **2000**, 1781.

(38) (a) Miller, J. S.; Krusic, P. J.; Dixon, D. A.; Reiff, W. M.; Zhang, J. H.; Anderson, E. C.; Epstein, A. J. *J. Am. Chem. Soc.* **1986**, *108*, 4459. (b) Mayerle, J. J.; Torrance, J. B. *Bull. Chem. Soc. Jpn.* **1981**, *54*, 3170.

(39) Lü, J.-M.; Rosokha, S. V.; Kochi, J. K. *J. Am. Chem. Soc.* **2003**, *125*, 12161.

(40) (a) Gillespie, R. J.; Kapoor, R.; Faggiani, R.; Lock, C. J. L.; Murchie, M.; Passmore, J. *J. Chem. Soc., Chem. Commun.* **1983**, 8. (b) Faggiani, R.; Gillespie, R. J.; Lock, C. J. L.; Vekris, J. E. *Inorg. Chem.* **1988**, *27*, 4350. (c) Gillespie, R. J.; Passmore, J. *Acc. Chem. Res.* **1971**, *4*, 413. (d) Brownridge, S.; Cameron, T. S.; Du, H.; Knapp, C.; Koppe, R.; Passmore, J.; Rautiainen, J. M.; Schnockel, H. *Inorg. Chem.* **2005**, *44*, 1660. (e) Drews, T.; Koch, W.; Seppelt, K. *J. Am. Chem. Soc.* **1999**, *121*, 4379. (f) Arulsamy, N.; Bohle, D. S.; Imonigie, J. A.; Sagan, E. S. *Inorg. Chem.* **1999**, *38*, 2716.

(41) (a) Nandana, W. A. S.; Passmore, J.; White, P. S.; Wong, C.-M. *J. Chem. Soc., Chem. Commun.* **1982**, 1098. (b) Nandana, W. A. S.; Passmore, J.; White, P. S.; Wong, C.-M. *Inorg. Chem.* **1990**, *29*, 3529.

(42) Power, P. P. *Chem. Rev.* **2003**, *103*, 789.

magnetic susceptibility measurements. For $x = 2$ and 4, the diradicals formed weakly coupled radical dimers with thermally accessible excited triplet states, as proven by solid-state EPR and magnetic susceptibility measurements. The experimental and computational results indicate that these radical pairs may be considered as lying on the border between conventional closed-shell and open-shell systems. In the field of thiazyl radical chemistry, the radical pairs in solid **1**$[AsF_6]_2$ and **2**$[AsF_6]_2$ represent the second and third examples whose the magnitude of the $\pi^*-\pi^*$ interradical exchange interaction was experimentally determined. Such extensive studies on the singlet−triplet gaps combining solid-state EPR and magnetic measurements have only been done for a few related organic radical pairs (e.g., $[TCNQ^{\bullet-}]_2$[21,35,36] and $[TTF^{\bullet+}]_2$).[32] The exchange interactions in radical pairs (divided by two) are approximately a measure of the strength of the $\pi^*-\pi^*$ bonds. This is another way to obtain dimerization energies of radical dimers, which are not trivial to obtain.[4] The corresponding in situ dimerization energies of radical pairs in polymeric $\mathbf{1}^{2+}$ and $\mathbf{2}^{2+}$ would then be approximately −3 and −5 kJ mol^{-1}, respectively. Accordingly, the dimerization energy in the previously reported $[ClCNSSS]_2^{2+}$ [8a] dimer can be estimated to be approximately −11 kJ mol^{-1}. Thus the dimeric $[RCNSSS]_2^{2+}$ salts possess a wide range of dimerization energies that can be determined in situ, reflecting the novel bonding properties of such weak interactions.

Unlike **1**$[AsF_6]_2$ and **2**$[AsF_6]_2$, the magnetic data on **3**$[AsF_6]_2{\cdot}SO_2$ were consistent with the presence of monomeric diradicals in the solid state. Clearly, the electronic properties of the $-CNSSS^{\bullet+}$ rings in $\mathbf{1}^{2+}-\mathbf{3}^{2+}$are identical, and their different physical properties stem from the different packing motifs adopted by a particular derivative. This tendency was also noted in the structures of monomeric $RCNSSS^{\bullet+}$ (R = F_5C_2, Cl_3C, F_3C)[8c] radical cations on variation of the alkane substituent. On the other hand, the AsF_6^- salts of the halogen derivatives (R = Cl, Br, I)[8a] were found to be isomorphous, and the radical cations were dimeric. Fine interplay between drastically different packing motifs observed for $RCNSSS^{\bullet+}$ radical cations is responsible for the dichotomy exhibited by the series of diradicals $C_xF_{2x}(CNSSS)_2^{\bullet\bullet2+}$ ($x = 2-4$) in the solid state.

At present, the factors leading to formation of monomeric versus associated/dimeric structures for the $RCNSSS^{\bullet+}$ radical cations are not clear. It should be noted that the extensively studied $RCNSSN^{\bullet}$ heterocycle (altogether more than 40 derivatives known) still has some degree of unpredictability regarding the extent of association in the solid state.[1] To gain more understanding of such systems, with the solid-state structures very sensitive to the substituent effect, it is more logical to introduce slight modifications into a substituent group, for example, by modifying the alkane moiety[8c] or increasing a spacer size as in the series of $\mathbf{1}^{2+}-\mathbf{3}^{2+}$. Although not all the puzzles have yet been resolved, we believe that our observations provide more information on the variety of packing motifs present in the structures of the $RCNSSS^{\bullet+}$ radical cations, which will aid in the assessment of their potential as precursors to organic/main group magnetic materials.

Acknowledgment. Funding of this work was provided by NSERC (J.P., K.V.S., L.K.T.), EPSRC (R.M.K., E.J.L.M.), and NSF (M.E., C.P.L.). C.P.L. is grateful for grants from the NSF (IMR-0314773) and the Kresge Foundation toward the purchase of the SQUID magnetometer. We thank Dr. Saba Mattar (University of New Brunswick) for recording isotropic solution EPR spectra and Dr. Tareque Abedin at MUN (Memorial University of Newfoundland) for assisting with magnetic measurements of **1**$[AsF_6]_2$. We are also grateful to Dr. J. Mikko Rautiainen, Dr. Heikki M. Tuononen (University of Jyväskylä, Finland), and Dr. Friedrich Grein (University of New Brunswick) for helpful discussion concerning some computational details.

Supporting Information Available: Crystallographic data in CIF format, figures showing the anion in **1**$[AsF_6]_2$ and the optimized conformations of $\mathbf{1}^{2+}$, $\mathbf{2}^{2+}$, and $\mathbf{3}^{2+}$, tables giving the values of χ for **1**$[AsF_6]_2-$**3**$[AsF_6]_2$, experimental and calculated vibrational frequencies for **1**$[AsF_6]_2$, **2**$[AsF_6]_2$, and **3**$[AsF_6]_2{\cdot}SO_2$, and a figure showing the magnetic suseptibility versus temperature for **3**$[AsF_6]_2{\cdot}SO_2$. This material is available free of charge via the Internet at http://pubs.acs.org.

IC062475I